IMMUNOBIOLOGY

Brief report

Naturally occurring short splice variant of CYLD positively regulates dendritic cell function

*Cathy Cecilia Srokowski,[1] *Joumana Masri,[2] Nadine Hövelmeyer,[2] Anna Katharina Krembel,[1] Christine Tertilt,[1] Dennis Strand,[2] Karsten Mahnke,[3] Ramin Massoumi,[4] †Ari Waisman,[2] and †Hansjörg Schild[1]

[1]Institute for Immunology, and [2]First Department of Internal Medicine, Johannes Gutenberg University, Mainz, Germany; [3]Department of Dermatology, University of Heidelberg, Heidelberg, Germany; and [4]Department of Laboratory Medicine, Clinical Research Center, Lund University, Malmo, Sweden

Deubiquitination of NF-κB members by CYLD is crucial in controlling the magnitude and nature of cell activation. The role of the naturally occurring CYLD splice variant in dendritic cell (DC) function was analyzed using CYLD[ex7/8] mice, which lack the full-length CYLD (fl-CYLD) transcript and overexpress the short splice variant (sCYLD). Bone marrow–derived DCs from CYLD[ex7/8] mice display a hyperactive phenotype in vitro and in vivo and have a defect in establishing tolerance with the use of DEC-205–mediated antigen targeting to resting DCs. The combination of sCYLD overexpression and lack of flCYLD in CYLD[ex7/8] DCs leads to enhanced NF-κB activity accompanied by an increased nuclear translocation of the IκB molecule Bcl-3, along with nuclear p50 and p65. This suggests that, in contrast to flCYLD, sCYLD is a positive regulator of NF-κB activity, and its overexpression induces a hyperactive phenotype in DCs. (Blood. 2009;113:5891-5895)

Introduction

CYLD is a tumor suppressor gene that is mutated in familial cylindromatosis, an autosomal dominant predisposition to tumors of skin appendages.[1] CYLD removes lysine-63 polyubiquitin chains from distinct members of the NF-κB pathway[2-4] and mutations in CYLD dysregulate NF-κB activity.

Complete deletion of CYLD in mice (CYLD[ko]) renders them susceptible to skin tumors,[5] but the CYLD[ko] mice do not display alterations of the immune system, as we could show for B-[6] and T-cell development (A.W., N.H., S. Reissig, manuscript in preparation). Other knockout mouse models of CYLD point to a role for flCYLD in immunity, including hyperinduction of IFNα in virus-infected dendritic cells (DCs)[7] as well as protection from infections in its absence.[8]

However, mice exclusively expressing the naturally occurring short splice variant of CYLD, sCYLD, are characterized by lymphomegaly, splenomegaly, and dramatic increases in B-cell numbers[6] caused by aberrant NF-κB signaling. Because this pathway is important for the function of DCs,[9] which orchestrate innate and adaptive immune responses, we investigated the effect of sCYLD overexpression on DC function. We found CYLD[ex7/8] DCs to be hyperresponsive to LPS, capable of inducing superior T-cell expansion on DC immunization in vivo, and able to suppress tolerance induced by α-DEC-205:OVA administration. As a molecular basis for this phenotype, we identified increased nuclear Bcl-3, p50, and p65 in resting and stimulated CYLD[ex7/8] bone marrow–derived DCs (BMDCs).

Methods

Mice and BMDC generation

C57BL/6 wild-type (WT), CYLD[ko],[5] and CYLD[ex7/8 6] mice 6 to 8 weeks old were used as recipients and for BMDC generation as previously described.[10] St42 TCR Tg mice have been previously described.[11] OT-I mice[12] were obtained from Christian Kurts (Institute for Molecular Medicine & Experimental Immunology, Bonn, Germany). Approval for these studies was obtained from the review board of the Federal State of Rhineland-Palatinate, Germany. All animal experiments were in accordance with the guidelines of the Central Animal Facility Institution of the University of Mainz.

Flow cytometry

FACSCanto cytometer and FlowJo software (Tree Star, Ashland, OR) using α-CD8 and α-CD90.1/CD45.1 (eBioscience, San Diego, CA) was used. α–IL-6, IL-10, and TNF-α antibodies from Cytometric Bead Array Flex system (Becton Dickinson, Franklin Lakes, NJ) were used and analyzed with FCAP Array Software (BD Biosciences, Mountain View, CA).

Immune tolerance

Recipient mice were given 10^6 adoptively transferred OT-I cells, immunized with 20 μg DEC-205:OVA, and boosted with 50 μg OVA protein (Sigma-Aldrich, St Louis, MO) as previously described.[13]

Western blot analysis and electrophoretic mobility shift assay

Western blot analysis was performed as previously described.[8] Nuclear and cytoplasmic fractions were prepared according to standard procedures.[14,15] NF-κB Consensus Oligonucleotide was purchased from

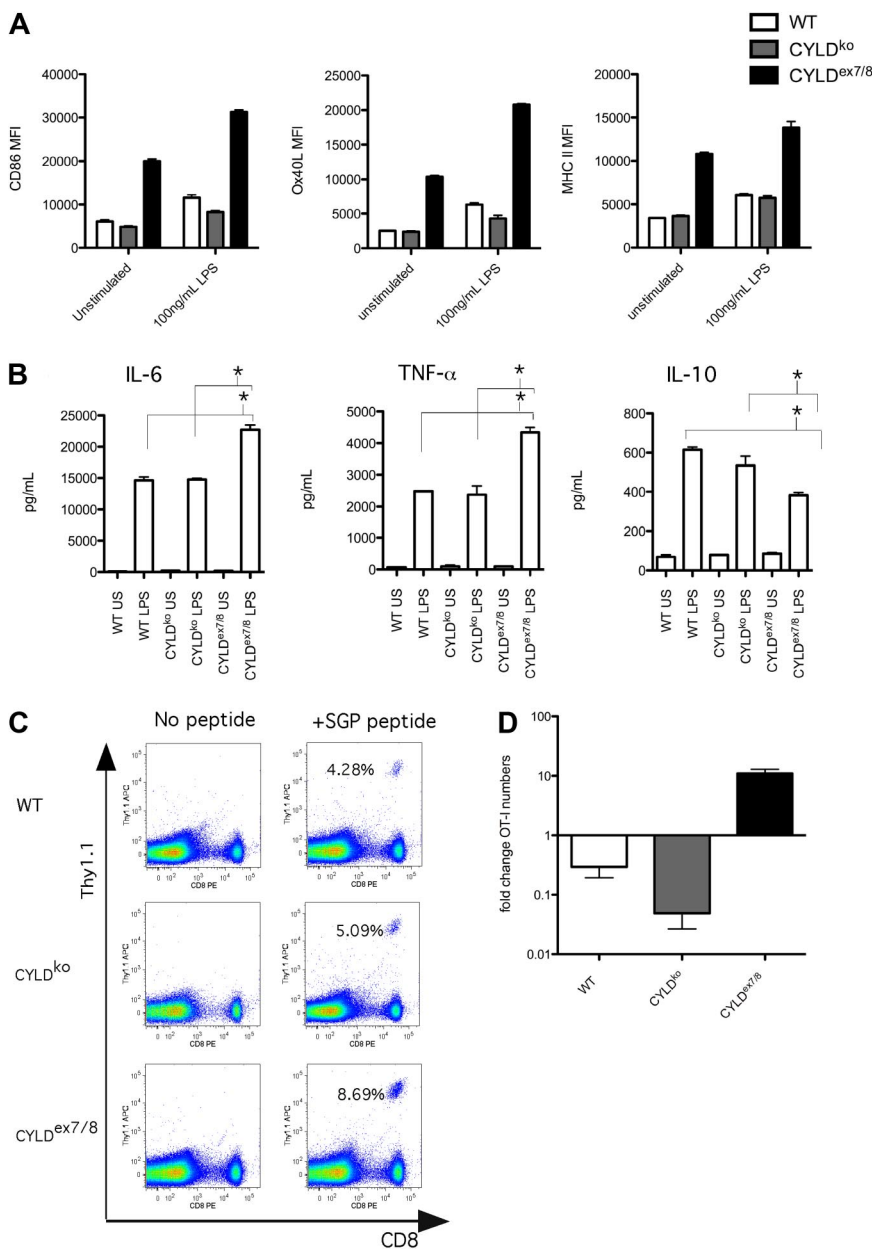The online version of this article contains a data supplement.

Figure 1. sCYLD confers a stimulatory phenotype in BMDCs that leads to T-cell expansion and suppression of tolerance upon α-DEC-205:OVA administration. (A) BMDCs from WT, CYLD[ko], and CYLD[ex7/8] mice were differentiated with GM-CSF for 6 days in culture and stimulated (100 ng/mL LPS, 12 hours) and submitted to fluorescence-activated cell sorting (FACS) analysis of the CD11c^{+} population and cell surface expression of CD86, MHC II, and Ox40L. Mean fluorescence intensity (MFI) values of indicated cell surface expression markers are representative of more than 10 BMDCs preparations with triplicates and SEM shown as error bars. (B) Supernatants from stimulated BMDCs cultures measured for IL-10, TNF-α, and IL-6 cytokines with Becton Dickinson CBA Flex Set System. *$P < .05$ using t test for WT compared with CYLD[ex7/8] and for CYLD[ko] compared with CYLD[ex7/8] stimulated BMDCs. Values shown are means of triplicates with SEMs. (C) Day 3 analysis of blood T-cell expansion of adoptively transferred TCR tg (St42) donor splenocytes into WT recipient mice immunized with day 6–differentiated and LPS-stimulated WT, CYLD[ko], or CYLD[ex7/8] BMDCs SGP peptide loaded and injected intraperitoneally to recipient WT mice. Percentages indicate Thy1.1^{+} CD8^{+} cells. Values are representative of more than 4 mice per group and repeated 3 times. (D) Fold change in OT-I T-cell numbers compared with PBS control in the spleen of recipient mice adoptively transferred with OT-I cells, given 20 μg DEC-205:OVA intra footpad and challenged with 50 μg OVA protein in CFA subcutaneously. Cell detection was analyzed by FACS using CD45.1 and CD8 antibodies to detect OT-I CD45.1 cells gated on CD8. Values represent more than 4 mice per group, with mean values and SEMs.

Promega (Madison, WI). Western blots and electrophoretic mobility shift assay (EMSA) were performed with antibodies α-p50 (Assay Designs, Ann Arbor, MI), α-Bcl-3 (Santa Cruz Biotechnology, Santa Cruz, CA), α–β-actin (Sigma-Aldrich), α-p65, and α-HDAC1 (Cell Signaling Technology, Danvers, MA).

Cell transfection and NF-κB luciferase reporter assay

Fibroblasts were transfected with sCYLD plasmid, using the Nucleofector Kit (Amaxa:VPD-1005; Amaxa Biosystems, Gaithersburg, MD). The NF-κB–Reporter plasmid was provided by Ralf Marienfeld[16] (Institute for Molecular Pathology, Wurzburg, Germany) and cotransfected with pRL-TK (Promega) into BMDCs with the Nucleofector Kit (VPA-1011; Amaxa). Luciferase reporter activity was analyzed as previously described.[17]

Quantitative real-time polymerase chain reaction

mRNA detection was performed as previously described[18] with Bcl-3 forward, TGCCCATTTACTCTACCCCGACGA; Bcl-3 reverse, CAGCGATGTG-

GAGAGGCGTGTC; sCYLD forward, CTATTGGCAACTGGGATGGAAGG; and sCYLD reverse, CACTTAAATAGCCCCCAAATGCTTC.

Statistical analysis

Values represent means plus or minus SEMs analyzed with the t test or 1-way ANOVA (analysis of variance).

Results and discussion

To analyze the role of CYLD and its naturally occurring short splice variant in DC function, we generated BMDCs and observed that immature CD11c^{+} BMDCs from CYLD[ex7/8] mice express higher levels of CD86, MHC II, and OX40L compared with WT or CYLD[ko] mice BMDCs (Figure 1A). sCYLD increase could be observed in WT DCs on stimulation (Figure S1A, available on the *Blood* website; see the Supplemental Materials link at the top of the online article), suggesting a role for sCYLD in DC function.
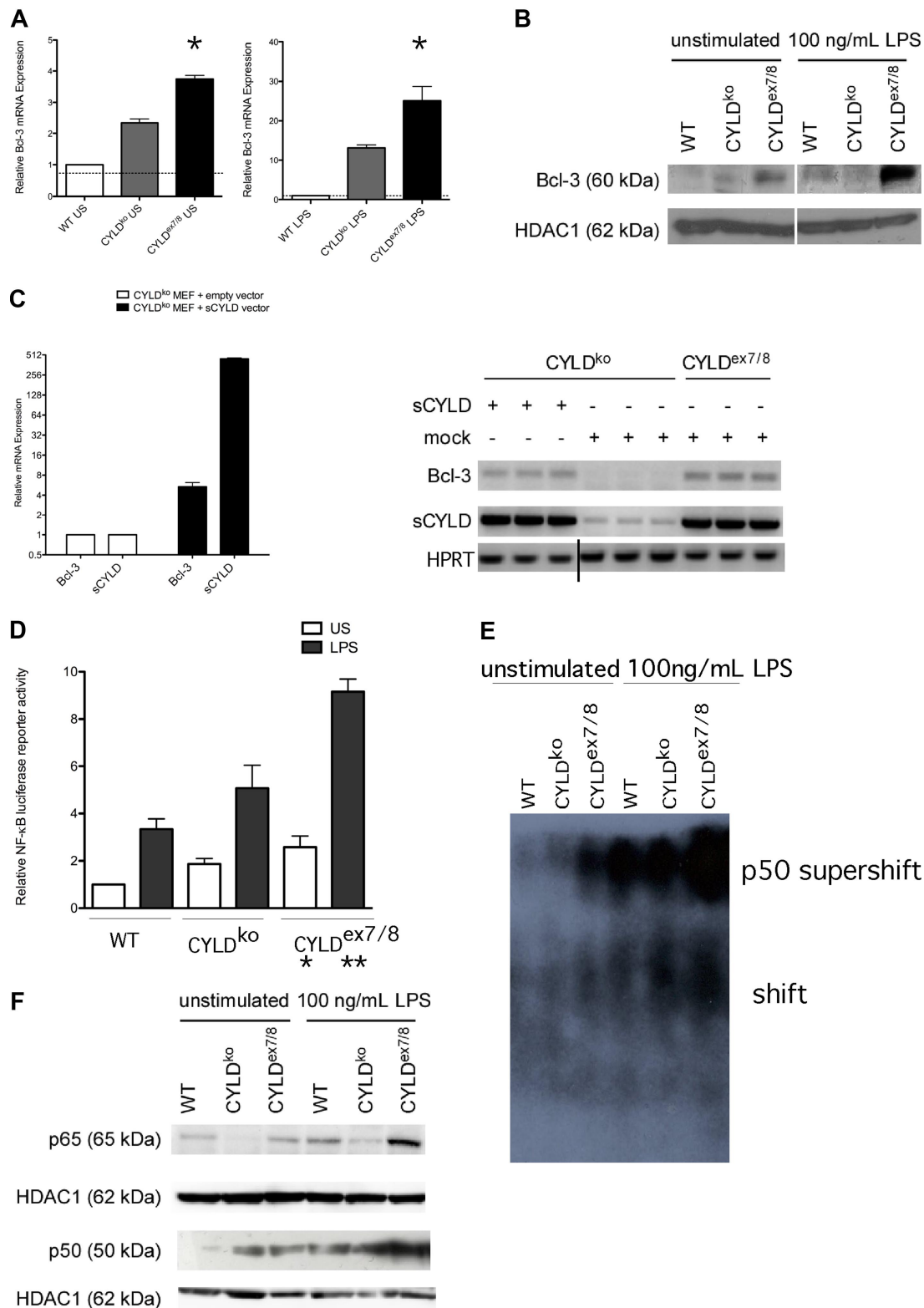
Figure 2. Analysis of NF-κB signaling in CYLD^ex7/8 BMDCs. (A) Differentiated day 6 WT BMDCs were stimulated (100 ng/mL LPS, 12 hours) or left untreated, and quantitative real-time–polymerase chain reaction (qRT-PCR) was performed to detect mRNA levels of Bcl-3. mRNA levels were normalized by HPRT levels and expressed as fold change. (B) Nuclear BMDC extracts from unstimulated and stimulated (100 ng/mL LPS, 12 hours) were examined by Western blotting using anti–Bcl-3. Shown are lysates from WT, CYLD^ko, and CYLD^ex7/8 mice. HDAC1 antibody was used as a loading control. (C) CYLD^ko mouse embryonic fibroblasts (MEFs) cells were transfected with empty vector or with sCYLD vector. Comparison of Bcl-3 up-regulation when sCYLD is expressed in CYLD^ko MEFs compared with mock-transfected CYLD^ko (bar graph). Gel represents the qRT-PCR products obtained after performance of qRT-PCR on sCYLD-transfected or mock-transfected MEFs as indicated in figure. Vertical line has been inserted to indicate a repositioned gel lane. (D) NF-κB luciferase reporter activity of BMDCs transfected with a NF-κB luciferase reporter construct untreated or stimulated (LPS 100 ng/mL, 12 hours). Cells were lysed after 24 hours, and luciferase activity was measured by a luminometer (Berthold Technologies, Bad Wildbad, Germany) using the dual luciferase reporter assay system from Promega. Data were standardized according to the *Renilla* luciferase activity and normalized to represent fold differences. *$P < .05$ using 1-way ANOVA between unstimulated samples; **$P < .05$ using 1-way ANOVA between LPS-stimulated samples. Panels A, C and D: Data represent mean values with standard mean error bars. (E) EMSA was performed with nuclear extracts from BMDCs that were unstimulated or stimulated with 100 ng/mL LPS for 12 hours and subsequently incubated with NF-κB–specific labeled probe and p50 antibody to perform supershift, and separated by native polyacrylamide gel electrophoresis (PAGE). (F) Nuclear BMDC extracts from unstimulated and stimulated (100 ng/mL LPS, 12 hours) were examined by Western blotting using anti-p50 and anti-p65. Shown are lysates from WT, CYLD^ko, and CYLD^ex7/8 mice. HDAC1 antibody was used as a loading control.

However, neither WT mice nor heterozygous CYLD[ex7/8] (WT/CYLD[ex7/8]) mice display a hyperactive BMDC phenotype (Figure S1B), indicating that a certain threshold level of sCYLD expression is required for the hyperactive phenotype.

On LPS stimulation, CYLD[ex7/8] BMDCs further amplify cell surface markers (Figure 1A) and secrete increased levels of the proinflammatory cytokines IL-6 and TNF-α but less of the anti-inflammatory cytokine IL-10 compared with WT BMDCs (Figure 1B).

To understand the in vivo consequences of CYLD[ex7/8] BMDC hyperactivity, BMDCs were stimulated with LPS, loaded with SGP peptide, and injected into WT mice, which received an adoptive transfer of SGP peptide-specific St42 TCR transgenic T cells. We observed a significantly higher expansion of the transferred T cells when the stimulation occurred via BMDCs from CYLD[ex7/8] mice, compared with BMDCs prepared from the other mice (Figure 1C). Because of the hyperactive phenotype of immature CYLD[ex7/8] BMDCs, we analyzed the capacity of these mice to induce T-cell tolerance in comparison to WT or CYLD[ko] animals. We injected α-DEC-205:OVA (which delivers ovalbumin in a steady state to DEC-205–expressing DCs[13]) to recipient mice adoptively transferred with OT-I cells. On challenge with ovalbumin in CFA, the OT-I T-cell population in the spleens of WT and CYLD[ko] recipient mice displayed, as expected, a strong reduction in OT-I T-cell numbers, whereas in CYLD[ex7/8] mice the OT-I cells expanded more than 10-fold (Figure 1D). This finding suggests that CYLD[ex7/8] mice lack the capacity for DC-mediated induction of tolerance toward exogenous antigens because of their predisposed high activation status.

To understand the mechanism behind our phenotypic observations, we focused on NF-κB members involved in CYLD-influenced NF-κB signaling. Bcl-3 has recently been shown to interact with both flCYLD and sCYLD and to modulate NF-κB activity.[5,8] Therefore, we investigated Bcl-3 expression and observed a significant increase on both the mRNA and nuclear protein level in CYLD[ex7/8] BMDCs compared with WT and CYLD[ko] (Figures 2A,B, S1C). To clarify the effect of sCYLD on Bcl-3 expression, we transfected CYLD[ko] fibroblasts with a sCYLD encoding plasmid and observed a 5-fold increase in Bcl-3 expression compared with mock-transfected CYLD[ko] cells (Figure 2C).

The enhanced Bcl-3 expression corresponded to higher NF-κB reporter activity in CYLD[ex7/8] BMDCs, which could already be observed in the unstimulated state (Figure 2D). To determine the NF-κB subunits involved, we turned to the well-known binding partner of Bcl-3, p50,[19,20] to assess its role in the observed NF-κB activation. Unstimulated CYLD[ex7/8] BMDCs displayed detectable NF-κB activation driven by p50 as shown by the supershifted complex in the EMSA (Figure 2E), which was not observed in WT or CYLD[ko] BMDCs. On stimulation, NF-κB activity increased in all cell types, but the degree of increase was most profound in CYLD[ex7/8] BMDCs. The aforementioned observation of p50-driven NF-κB activation turned our interest to its most common and best-characterized binding partner, p65, which together with p50 forms a heterodimer p50/p65 that is known to activate gene transcription.[21,22] The increased nuclear p65 and p50 protein levels

concomitant with decreased cytoplasmic p105 expression in resting and stimulated CYLD[ex7/8] BMDCs compared with WT and CYLD[ko] (Figures 2F, S1D) suggest that the increased NF-κB activation in these cells is a result of sCYLD overexpression.

Although resting CYLD[ko] BMDCs express higher Bcl-3 mRNA and protein levels compared with WT BMDCs, they do not display a hyperactive phenotype (Figure 2B). Moreover, overexpression of Bcl-3 in WT BMDCs caused only a minimal up-regulation of the surface marker CD86 (Figure S1E), supporting a model in which, only when sCYLD is overexpressed and flCYLD is absent, does the up-regulation of Bcl-3 followed by its nuclear translocation, correspond to a hyperactive phenotype. The interplay between sCYLD and Bcl-3 could further be verified by showing that nuclear Bcl-3 localization occurs exclusively in the presence of sCYLD and the absence of its full-length transcript (Figure S1F).

Taken together we propose a model in which the exclusive overexpression of sCYLD with high nuclear levels of Bcl-3 in BMDCs is accompanied by an increased NF-κB activation, resulting in a hyperactive phenotype. These results propose a stimulatory role for sCYLD and indicate that the relationship between flCYLD and sCYLD needs further investigation to deepen our understanding of deubiquitinating enzymes in NF-κB signaling and their distinct roles in positive and negative regulation.

Authorship

Contribution: C.C.S., J.M., and A.K.K. performed experiments; C.C.S. and J.M. created the figures; C.C.S., J.M., C.T., A.W., and H.S. designed the research; C.C.S. and J.M. analyzed and interpreted the data; D.S. provided useful technical expertise; C.C.S., J.M., A.W., N.H., and H.S. wrote the paper; and R.M. and K.M. provided valuable reagents.

Conflict-of-interest disclosure: The authors declare no competing financial interests.

Correspondence: Ari Waisman, First Medical Department, Johannes Gutenberg University Mainz, Verfügungsgebäude, D-55131, Mainz, Germany; e-mail: waisman@uni-mainz.de; or Hansjörg Schild, Institute for Immunology, Johannes Gutenberg University, Obere Zahlbacher Str 67, D-55131 Mainz, Germany; e-mail: schild@uni-mainz.de.

References

1. Bignell GR, Warren W, Seal S, et al. Identification of the familial cylindromatosis tumour-suppressor gene. Nat Genet. 2000;25:160-165.

2. Trompouki E, Hatzivassiliou E, Tsichritzis T, Farmer H, Ashworth A, Mosialos G. CYLD is a deubiquitinating enzyme that negatively regulates NF-kappaB activation by TNFR family members. Nature. 2003;424:793-796.

3. Brummelkamp TR, Nijman SM, Dirac AM, Bernards R. Loss of the cylindromatosis tumour suppressor inhibits apoptosis by activating NF-kappaB. Nature. 2003;424:797-801.

4. Kovalenko A, Chable-Bessia C, Cantarella G, Israel A, Wallach D, Courtois G. The tumour suppressor CYLD negatively regulates NF-kappaB signalling by deubiquitination. Nature. 2003;424: 801-805.

5. Massoumi R, Chmielarska K, Hennecke K,

Pfeifer A, Fassler R. Cyld inhibits tumor cell proliferation by blocking Bcl-3-dependent NF-kappaB signaling. Cell. 2006;125:665-677.

6. Hovelmeyer N, Wunderlich FT, Massoumi R, et al. Regulation of B cell homeostasis and activation by the tumor suppressor gene CYLD. J Exp Med. 2007;204:2615-2627.

7. Zhang M, Wu X, Lee AJ, et al. Regulation of IkappaB kinase-related kinases and antiviral responses by tumor suppressor CYLD. J Biol Chem. 2008;283:18621-18626.

8. Lim JH, Stirling B, Derry J, et al. Tumor suppressor CYLD regulates acute lung injury in lethal Streptococcus pneumoniae infections. Immunity. 2007;27:349-360.

9. Ouaaz F, Arron J, Zheng Y, Choi Y, Beg AA. Dendritic cell development and survival require distinct NF-kappaB subunits. Immunity. 2002;16:257-270.

10. Warger T, Osterloh P, Rechtsteiner G, et al. Synergistic activation of dendritic cells by combined Toll-like receptor ligation induces superior CTL responses in vivo. Blood. 2006;108:544-550.

11. Rechtsteiner G, Warger T, Hofmann M, Rammensee HG, Schild H, Radsak MP. Precursor frequency can compensate for lower TCR expression in T cell competition during priming in vivo. Eur J Immunol. 2006;36:2613-2623.

12. Hogquist KA, Jameson SC, Heath WR, Howard JL, Bevan MJ, Carbone FR. T cell receptor antagonist peptides induce positive selection. Cell. 1994;76:17-27.

13. Bonifaz L, Bonnyay D, Mahnke K, Rivera M, Nussenzweig MC, Steinman RM. Efficient targeting of protein antigen to the dendritic cell receptor DEC-205 in the steady state leads to antigen presentation on major histocompatibility complex class I products and peripheral CD8+ T cell tolerance. J Exp Med. 2002;196:1627-1638.

14. Weih F, Carrasco D, Bravo R. Constitutive and inducible Rel/NF-kappa B activities in mouse thymus and spleen. Oncogene. 1994;9:3289-3297.

15. Schreiber E, Matthias P, Muller MM, Schaffner W. Rapid detection of octamer binding proteins with 'mini-extracts', prepared from a small number of cells. Nucleic Acids Res. 1989;17:6419.

16. Suhasini M, Reddy CD, Reddy EP, DiDonato JA, Pilz RB. cAMP-induced NF-kappaB (p50/relB) binding to a c-myb intronic enhancer correlates with c-myb up-regulation and inhibition of erythroleukemia cell differentiation. Oncogene. 1997;15:1859-1870.

17. Stassen M, Klein M, Becker M, et al. p38 MAP kinase drives the expression of mast cell-derived IL-9 via activation of the transcription factor GATA-1. Mol Immunol. 2007;44:926-933.

18. Bopp T, Palmetshofer A, Serfling E, et al. NFATc2 and NFATc3 transcription factors play a crucial role in suppression of CD4+ T lymphocytes by CD4+ CD25+ regulatory T cells. J Exp Med. 2005;201:181-187.

19. Fujita T, Nolan GP, Liou HC, Scott ML, Baltimore D. The candidate proto-oncogene bcl-3 encodes a transcriptional coactivator that activates through NF-kappa B p50 homodimers. Genes Dev. 1993;7:1354-1363.

20. Nolan GP, Fujita T, Bhatia K, et al. The bcl-3 proto-oncogene encodes a nuclear I kappa B-like molecule that preferentially interacts with NF-kappa B p50 and p52 in a phosphorylation-dependent manner. Mol Cell Biol. 1993;13:3557-3566.

21. Siebenlist U, Franzoso G, Brown K. Structure, regulation and function of NF-kappa B. Annu Rev Cell Biol. 1994;10:405-455.

22. Baldwin AS Jr. The NF-kappa B and I kappa B proteins: new discoveries and insights. Annu Rev Immunol. 1996;14:649-683.